Am. J. Hum. Genet. 63:1294–1306, 1998

Phenotype-Genotype Relationships in Complementation Group 3 of the Peroxisome-Biogenesis Disorders

Chia-Che Chang and Stephen J. Gould

Department of Biological Chemistry, The Johns Hopkins University School of Medicine, Baltimore

Summary

The peroxisome-biogenesis disorders (PBDs) are a set of often lethal genetic diseases characterized by mental retardation and defective peroxisomal matrix protein import. Mutations in *PEX12* are known to underlie the disease in two patients from complementation group 3 of the PBDs. Here we show that all patients from this group carry mutations on both alleles of *PEX12*. A comparison between *PEX12* genotypes and the clinical and cellular phenotypes of the corresponding PBD patients suggests a relatively straightforward relationship between genotype and phenotype in this group of the PBDs, such that the loss of *PEX12* function leads to more-severe cellular and clinical phenotypes. However, one patient who presented relatively mild clinical and cellular phenotypes was a compound heterozygote for two seemingly severe mutations on each *PEX12* allele. PEX12 mRNA present in the patient's cells was derived from only one allele, the one that carried a 2-bp deletion early in the *PEX12* coding region, c.26,27Δ. The deduced protein product of this mRNA would contain only the first eight amino acids of the protein, and yet this mutant PEX12 cDNA displayed significant *PEX12* activity in a functional complementation assay. Surprisingly, the PEX12/c.26,27Δ cDNA directed the synthesis of a 29-kD PEX12 protein in vitro, a result that is consistent with translation initiation at a downstream AUG codon. Transfection studies confirmed the expression of similarly sized PEX12 proteins from the *PEX12*/c.26,27Δ allele. Thus, it appears that translation initiation at internal AUG codons may modulate disease phenotypes and should be considered whenever unexpectedly mild phenotypes result from severe mutations early in the coding region.

Received April 28, 1998; accepted for publication September 16, 1998; electronically published October 23, 1998.

Address for correspondence and reprints: Dr. Stephen J. Gould, Associate Professor, Department of Biological Chemistry, The Johns Hopkins University School of Medicine, 725 North Wolfe Street, Baltimore, MD 21205. E-mail: Stephen.Gould@qmail.bs.jhu.edu

0002-9297/98/6305-0007$02.00

Introduction

Two distinct clinical spectra have been recognized within the peroxisome-biogenesis disorders (PBDs). One is composed of Zellweger syndrome (ZS), neonatal adrenoleukodystrophy (NALD), and infantile Refsum disease (IRD) and is referred to as "the Zellweger spectrum." Within the Zellweger spectrum of disease, ZS is the most severe and is typified by neurological, hepatic, and renal abnormalities, pronounced mental retardation, and death in early infancy. NALD patients display a generally less severe and more restricted set of phenotypes, and IRD phenotypes are even milder. There are at least nine complementation groups (CGs) of Zellweger-spectrum patients (Shimozawa et al. 1993), but there is no relationship between disease phenotype and CG. The other spectrum of phenotypes is typified by classical rhizomelic chondrodysplasia punctata (cRCDP) (Lazarow and Moser 1995) but also includes patients with milder phenotypic variations (Moser et al. 1995). In contrast to Zellweger-spectrum patients, cRCDP patients lie within a single CG and display proximal shortening of the long bones of the limbs and extensive punctate calcifications in addition to the severe neurological deficits and mental retardation observed in all PBD patients (Lazarow and Moser 1995).

All PBD patients display defects in multiple peroxisomal metabolic processes, and these result from an inability to import peroxisomal matrix proteins. Newly synthesized peroxisomal proteins are imported into peroxisomes posttranslationally and carry either of two peroxisomal targeting signals (PTSs) that are sufficient to direct them to and into the peroxisome: the PTS1 or the PTS2 (Subramani 1993). The fact that all Zellweger-spectrum patients exhibit a defect in PTS1-protein import and that all cRCDP patients display a selective defect in PTS2-protein import demonstrates that these two clinical spectra are heavily influenced by the specificity of these import pathways (Slawecki et al. 1995). The PTS1, a C-terminal tripeptide of the sequence ser-lys-leu-$_{COOH}$ (SKL) or a variant thereof, targets the majority of proteins to peroxisomes (Gould et al. 1989). This includes the enzymes acyl-CoA oxidase and D-specific hydratase/dehydrogenase, the enzymes defective in two

diseases with clinical symptoms similar to ZS, pseudo-NALD (Poll-The et al. 1988) and pseudo-ZS (Suzuki et al. 1997), respectively. In contrast to the PTS1, the PTS2 (Swinkels et al. 1991) is found at or near the N-terminus of proteins, consists of the sequence RLX_5HL, and targets only a few proteins to peroxisomes. In fact, only three PTS2-containing proteins are known in humans: thiolase (Swinkels et al. 1991), phytanoyl-CoA α-hydroxylase (PAHX) (Jansen et al. 1997; Mihalik et al. 1997), and alkyl-dihydroxyacetonephosphate synthase (de Vet et al. 1997). Integral peroxisomal membrane proteins use neither a PTS1 nor a PTS2 but, rather, employ a distinct class of PTS (Dyer et al. 1996).

Peroxisomal protein import requires a diverse set of peroxisome-assembly factors, referred to as "peroxins." Studies on yeast- and mammalian-cell mutants defective in peroxisomal protein import have led to the identification of various peroxins involved in recognition, targeting, and translocation of proteins into peroxisomes. These peroxins include the PTS1 receptor PEX5, the PTS2 receptor PEX7, and 16 other peroxisome-associated proteins required for import of both PTS1 and PTS2 proteins (van der Klei and Veenhuis 1997). To date, 14 human *PEX* genes have been identified, including the genes mutated in PBD patients representing CG1 (*PEX1;* Portsteffen et al. 1997; Reuber et al. 1997), CG2 (*PEX5;* Dodt et al. 1995), CG3 (*PEX12;* Chang et al. 1997; Okumoto and Fujiki 1997), CG4 (*PEX6;* Fukuda et al. 1996; Yahraus et al. 1996), CG7 (*PEX10;* Warren et al. 1998), CG10 (*PEX2;* Shimozawa et al. 1992), and CG11 (*PEX7;* Braverman et al. 1997; Motley et al. 1997; Purdue et al. 1997). During our initial characterization of human *PEX12,* we identified inactivating mutations on both alleles of *PEX12* in two unrelated ZS patients from CG3 (Chang et al. 1997). In the present study, we identified the mutations in all five remaining CG3 patients and characterized the cellular phenotypes of all seven CG3 patients. Our results provide insights into *PEX12* function, phenotype-genotype relationships in the PBDs, and the possible modification of disease phenotypes by translation initiation at internal ATG codons.

Material and Methods

Cell Lines and Strains

Human skin fibroblast-cell lines from unaffected individuals were obtained from the Coriell Cell Repository (Camden, NJ). Skin fibroblasts from PBD patients were obtained from Ann and Hugo Moser (The Kennedy Krieger Institute, Baltimore). All fibroblasts were cultured in complete medium (Dulbecco's modified Eagle's medium-high glucose [Dulbecco's minimal essential medium] supplemented with 10% fetal bovine serum and penicillin/streptomycin). Transformed derivatives of human skin fibroblast cells were generated by transfection with the plasmid pRSV-SV40T, followed by selection for transformed foci (Dodt et al. 1995). All PBD cell lines are referred to by patient number. All bacterial manipulations were performed with the *Escherichia coli* strain DH10B (Grant et al. 1990).

Northern Blot Analysis and Mutation Detection

RNA was isolated from cultured skin fibroblasts by use of PUREscript reagents and protocols (Gentra Systems). For northern analysis, 20 μg of total RNA from each cell line was separated by denaturing agarose-gel electrophoresis, transferred to GeneScreen filters (NEN Life Sciences), and hybridized first with a radiolabeled *PEX12* cDNA probe (including the entire open reading frame [ORF]) and subsequently with a radiolabeled β-actin cDNA probe. Levels of each mRNA were inferred from autoradiography of x-ray film and by phosphorimage analysis by use of a Fuji MacBAS phosphorimager.

The *PEX12* sequence was examined at the level of genomic DNA. Genomic DNAs were extracted from skin fibroblasts by use of the TurboGen kit (Invitogen). One hundred nanograms of each sample was used as the template for amplification of a 2.3-kb fragment of the *PEX12* gene by use of the oligonucleotides Chang-21 (5′-CAAGGTACCAAGTGAAAGCCAGTACACG-CAG-3′) at the 5′ end and Chang-20 (5′-CCAG-GATCCGTGAGGATAAGACATGATTCCC-3′) at the 3′ end. In all cases, the PCR products were sequenced directly. All mutations were also examined by allele-specific oligonucleotide (ASO) hybridization (Michaud et al. 1992). In brief, the 2.3-kb *PEX12*-gene fragment was amplified from each patient, transferred to GeneScreen filters, and hybridized with end-labeled oligonucleotides (14 nucleotides long) corresponding to the wild-type and mutant gene sequences. For ASO hybridization analysis, the oligonucleotides 5′-CTAGATCTTCTGCT-3′ and 5′-TGCTAGATCTGCTC-3′ were used to discriminate between the wild-type and mutant sequence of PBD095, the oligonucleotides 5′-GCTTAAAGAGAATT-3′ and 5′-CGGCTTAGAATTGT-3′ were used to discriminate between the wild-type and mutant sequence of PBD096, and the oligonucleotides 5′-ACTTCACAGCTGCT-3′ and 5′-CACTTCAGCTGCTT-3′ were used to discriminate between the wild-type and mutant sequence of the PBD099 c.26,27Δ allele.

Mutation analysis was also performed at the cDNA level. First-strand *PEX12* cDNA was synthesized by use of Superscript RT (Life Technologies), 10 μM *PEX12*-specific primer (5′-GTCTTGCTACCACCTCACTGTT-CAC-3′, located in the 3′ UTR), and 5 μg of total RNA in a volume of 25 μl. A *PEX12* cDNA fragment spanning the entire ORF but lacking most of the 5′ UTR was

amplified from 2.5 μl of first-strand cDNA by use of the oligonucleotides Chang-21 at the 5′ end and Chang-20 at the 3′ end. A *PEX12* cDNA fragment spanning the entire ORF as well as the 5′ UTR was amplified from 2.5 μl of first-strand cDNA by use of the oligonucleotides Chang-120 at the 5′ end and Chang-20 at the 3′ end. PCR products were gel purified and sequenced directly.

Plasmids and 5′ Rapid Amplification of cDNA Ends (RACE)

We have already described plasmids designed to express the *PEX12* cDNA (pcDNA3-*PEX12*), the *PEX12myc* cDNA (pcDNA3-*PEX12*myc) (Chang et al. 1997), and the *PAHXmyc* cDNA (Mihalik et al. 1997). The plasmid designed to express the *PEX12* gene, pCC037, was created by amplifying the *PEX12* gene from genomic DNA of an unaffected individual by use of the oligonucleotides Chang-21 and Chang-20, followed by subcloning the resulting 2.3-kb fragment between the *Asp*718 and *Bam*HI sites of pcDNA3. Plasmids containing all *PEX12* alleles from all seven CG3 patients were created in an analogous manner. Recombinant techniques were used to remove PCR-generated mutations from subclones of each allele, ensuring that the *PEX12* gene accurately reflected the sequence of each allele. The *PEX12*/c.26,27Δ cDNA was generated, by reverse transcription–PCR (RT-PCR), from PBD099 RNA as described above, followed by cleavage of the cDNA fragment with *Asp*718 and *Bam*HI and insertion of this fragment between the *Asp*718 and *Bam*HI sites of pcDNA3, creating pcDNA3-*PEX12*/c.26,27Δ (the only cDNA detected in this patient is derived from this allele). Sequence analysis confirmed that the deletion of nucleotides 26 and 27 of the ORF were the only mutations in the *PEX12* segment of this plasmid. The myc-tagged version of *PEX12*/c.26,27Δ cDNA was generated by recombining the 5′ end of this cDNA with the 3′ end of the *PEX12myc* cDNA. The *PEX12*/1-93Δ cDNA was created by transferring the 1,357-bp-long *Bgl*II-*Xho*I fragment from pcDNA3-*PEX12* into the *Bam*HI and *Xho*I restriction-enzyme sites of pcDNA3, deleting the first 66 codons of the *PEX12* ORF and all of the 5′ UTR of the *PEX12* cDNA, and leaving M94 as the first in-frame ATG codon. The myc-tagged version of the *PEX12*/1-93Δ cDNA was created by removing the 1,747-bp *Sma*I fragment of pcDNA3-*PEX12*/1-93Δ and replacing it with the analogous *Sma*I fragment of pcDNA3-*PEX12myc*. Additional expression vectors designed to express *PEX12* cDNA products of other mutant alleles were generated in a manner analogous to that for pcDNA3-*PEX12*/c.26,27Δ. For 5′-RACE amplification of the *PEX12* cDNA 5′ end, Marathon-Ready cDNA (Clontech) was used as the template, together with anchor primers supplied by the manufacturer and two *PEX12* gene–specific primers (5′-TTTGGGAGACCAGCACTAGC-3′ [*PEX12* RACE-3′] and 5′-TCAGCCATAGTTTCCTGCGTG-3′). After two rounds of amplification, a distinct band was detected, subcloned, and sequenced. The 5′ UTR was amplified from PEX12 cDNA and from genomic DNAs, by use of the oligonucleotides Chang-120 and *PEX12* RACE-3′. The *PEX12* cDNA and genomic DNA sequences in GenBank (accession numbers U91521 and U91522) have been modified to reflect this new information.

Transfections, Indirect Immunofluorescence, Antibodies, and Fluorescence Microscopy

Transfections were performed by electroporation (Chang et al. 1997). Cells were grown to 90% confluency in a 75-cm^2 flask, washed twice with 10 ml of HBS solution (21 mM HEPES, 137 mM NaCl, 5 mM KCl, 0.7 mM Na_2HPO_4, and 6 mM dextrose), resuspended in 0.5 ml HBS, and transferred to a 0.4-cm-gap sterile electroporation cuvette containing 10 μg DNA. After gentle mixing of the DNA and cell suspension, electroporation was performed in a BTX ECM600 electroporator (BTX) at 220–260 V, 1,500 μF, 129 ohms. After electroporation, cells were resuspended in 1 ml of complete medium, transferred to a 25-cm^2 flask, and incubated at 37°C. The medium was changed the next morning, and 2 d after transfection the cells were fixed, permeabilized, and processed for indirect immunofluorescence, as described elsewhere (Slawecki et al. 1995). Permeabilization was performed with 1% Triton X-100, which permeabilizes both plasma and peroxisome membranes. Rabbit polyclonal antibodies against the PTS1 tripeptide ser-lys-leu-$_{COOH}$ have been described elsewhere (Gould et al. 1990), as has the anti–c-myc mouse monoclonal antibody 1-9E10 (Evan et al. 1985). Rabbit polyclonal antibodies against c-myc, sheep anti–human catalase antibodies, and fluorescently labeled secondary antibodies were obtained from commercial sources.

Western Blot Analysis and In Vitro Translation of Proteins

Normal human fibroblast cells were transfected with pcDNA3, the pcDNA3-*PEX12myc* gene, and the pcDNA3-*PEX12myc*/c.26,27Δ gene. Two days after transfection, cell lysates were prepared from each of the three transfected cell populations by scraping the cells into lysis buffer (10 mM Tris, pH 7.8, 1% NP40, 0.15 M NaCl, 1 mM phenylmethylsulfonyl fluoride, and 1 mM EDTA), homogenizing the lysates, and subsequently spinning the lysates at 8,000 *g*, at 4°C for 5 min to remove the nuclei and cell debris. Proteins in the lysates were separated by SDS-PAGE, transferred to Immobilon-P transfer membrane (Millipore), probed with polyclonal anti–c-myc antibodies, and visualized by ECL

(Amersham Life Science), according to the manufacturer's protocol. *PEX12* proteins were synthesized in the presence of [^{35}S]-methionine, by use of the TNT lysate system (Promega), and were separated by SDS-PAGE. The gels were fixed, incubated in sodium salicylate, dried, and detected by fluorographic exposure of x-ray film. Coupled in vitro transcription and translation of PEX12 proteins from pcDNA3-based plasmids were possible because pcDNA3 carries a T7 promoter between the cytomegalovirus promoter and the *PEX12* cDNAs.

Results

Protein Import Phenotypes of PBD CG3 Cells

Our pool of PBD patients belonging to CG3 included five individuals who were diagnosed with ZS (PBD006, PBD040, PBD096, PBD097, and PBD098), one who was diagnosed with NALD (PBD095), and one who displayed the phenotypes of IRD (PBD099). As a first step toward defining the phenotype-genotype relationships in these cells, we examined the import of PTS1- and PTS2-containing proteins in skin fibroblasts that were derived from these seven CG3 patients. Import of PTS1-containing proteins was assayed by indirect immunofluorescence using anti-SKL antibodies, which recognize multiple PTS1-containing proteins (Gould et al. 1990). To assay PTS2-protein import, skin fibroblasts from each patient were transfected with a plasmid designed to express PAHXmyc, a C-terminally tagged version of the PTS2 protein PAHX (Mihalik et al. 1997). Two days after transfection, the cells were processed for indirect immunofluorescence, by use of anti-myc antibodies. We were unable to detect import of either PTS1 or PTS2 proteins in any of the cell lines derived from the five ZS patients (fig. 1*C* and *D*). However, cells from the NALD patient (PBD095) showed slight import of both PTS1- and PTS2-containing proteins (fig. 1*E* and *F*), and cells from the IRD patient (PBD099) exhibited even greater import of both classes of matrix proteins (fig. 1*G* and *H*).

PEX12 *Mutations in CG3 Patients*

The simplest model of phenotype-genotype relationships in the PBDs predicts that CG3 cell lines with milder defects in peroxisomal protein import would express some *PEX12* activity. To test this hypothesis, we first performed northern blot analysis on cells from all seven CG3 patients. The NALD and IRD lines, PBD095 and PBD099, had normal or nearly normal levels of *PEX12* mRNA, as did the ZS lines PBD040 and PBD097. However, the ZS lines PBD006, PBD096, and PBD098 contained reduced quantities of *PEX12* mRNA (fig. 2), which is a common consequence of nonsense and frameshift mutations (Maquat 1995).

We next determined the *PEX12*-gene sequence in the CG3 patients. The 1,077-bp ORF of *PEX12* is split by just two introns, of 305 and 857 bp. A 2.3-kb fragment of the *PEX12* gene, a fragment that includes all *PEX12* coding regions and short stretches of the 5′ and 3′ UTRs, was amplified from genomic DNA by PCR and was sequenced directly (fig. 3*A*–*C*). Mutations were also confirmed independently by ASO hybridization analysis of amplified genomic DNA (fig. 3*D*). In addition, all *PEX12* alleles were subcloned. Sequence analysis revealed that the two mutations identified in PBD006, PBD097, PBD098, and PBD099 were present on distinct alleles (data not shown) (Chang et al. 1997).

The five CG3 patients with the clinical diagnosis of ZS were all completely defective in peroxisomal matrix protein import (fig. 1). Not surprisingly, all of the mutations identified in these patients are expected to have a severe effect on gene function. PBD006 is a compound heterozygote for a G→T transversion at the splice-donor site of intron 1 and a C→T transition at nucleotide 538 of the ORF (fig. 3 and table 1), both of which appear to affect mRNA stability (of the CG3 patients whom we examined, PBD006 had the lowest *PEX12* mRNA levels). The first of these mutations would block removal of intron 1, leading to synthesis of only the first 42 amino acids of the protein and termination after incorporation of two additional amino acids. The second allele, R180ter, results in premature termination at the arginine 180 codon. PBD096, who also exhibited reduced *PEX12* mRNA levels, is homozygous for a 4-bp deletion (AAGA) of nucleotides 268–271 of the ORF, which shifts the reading frame. Its product is predicted to include the first 89 amino acids of PEX12 and to then terminate after the addition of two extra amino acids. PBD098 is a compound heterozygote for both a nonsense mutation, R180ter (the same as that in PBD006), and a 2-bp deletion of nucleotides 887–888 of the ORF, which changes the reading frame and leads to expression of just the first 296 amino acids, followed by addition of 11 extra amino acids before termination. As described in our previous report, ZS patient PBD040 is homozygous for a 4-bp deletion of nucleotides 684–687 of the ORF, truncating the protein at amino acid 228. ZS patient PBD097 is a compound heterozygote for a 4-bp insertion at nucleotide 733 (frameshift after amino acid 244 and termination after an additional 18 residues) and a 1-bp insertion at nucleotide 744 (frameshift after amino acid 248 and termination after an additional 14 amino acids).

We expected that, in contrast to the severe nonsense and frameshift mutations identified in the five ZS patients from CG3, the NALD and IRD patients would have milder mutations in *PEX12*. This was the case for

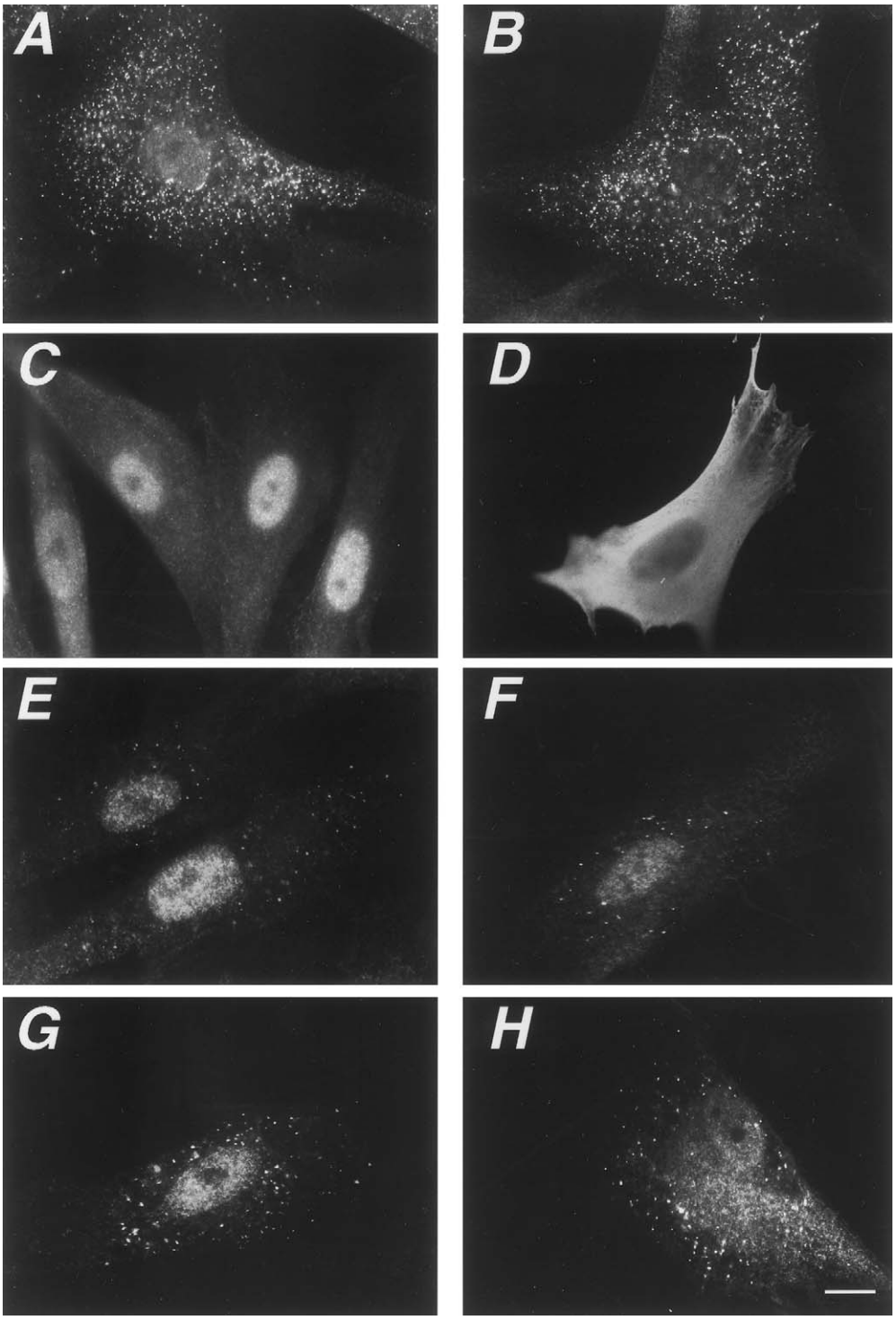

Figure 1 Subcellular distribution of peroxisomal proteins in PBD CG3 cell lines. The import of PTS1-containing peroxisomal proteins was assessed by indirect immunofluorescence, by use of anti-SKL antibodies (*A*, *C*, *E*, and *G*) in human skin fibroblasts from an unaffected individual, GM5756 (*A*); CG3 ZS patient PBD097 (*C*); the NALD patient, PBD095 (*E*); and the IRD patient, PBD099 (*G*). To assess the import of PTS2-containing proteins, we introduced the *PAHXmyc* expression vector into these same cell lines (*PAHX* encodes the PTS2-targeted peroxisomal enzyme PAHX, and PAHXmyc is targeted to peroxisomes by the PTS2 import pathway; Mihalik et al. 1997). The GM5756 cell expressing PAHXmyc imports the protein into peroxisomes (*B*), whereas no import is detected in ZS cell line PBD097 (*D*). A small amount of PTS2-protein import is detected in the NALD cell line, PBD095 (*F*), and even more import appears to occur in PBD099 cells (*H*). (Scale bar = 20 μm)

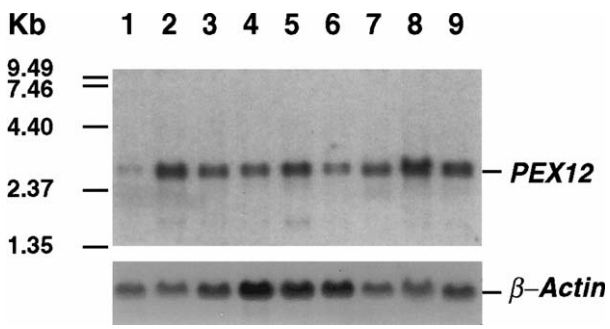

Figure 2 *PEX12* and actin mRNA levels in CG3 fibroblast cells. Total RNA was isolated from skin fibroblast-cell lines and was subjected to northern blot analysis using *PEX12* cDNA as probe. Lane 1, PBD006. Lane 2, PBD040. Lane 3, PBD095. Lane 4, PBD096. Lane 5, PBD097. Lane 6, PBD098. Lane 7, PBD099. Lane 8, GM5756 (unaffected individual). Lane 9, GM8333 (unaffected individual). The autoradiogram obtained after probing the northern blot with the *PEX12* cDNA probe is shown in the upper panel, and the size expected for the *PEX12* mRNA is noted on the right. The lower panel shows the level of β-actin mRNA. Quantization of *PEX12* mRNA abundance in each sample was performed by use of a Fuji phosphorimager.

the NALD patient, PBD095, who was homozygous for a 3-bp deletion that removed the Leu 68 codon (L68Δ) (fig. 3 and table 1). We found that expression of the L68Δ cDNA partially restored peroxisomal matrix protein import in cells from the severely affected ZS patient, PBD097, a result that is consistent with the hypothesis that this mutation does not completely eliminate *PEX12* function (data not shown). In contrast, we found that the most mildly affected patient, PBD099, was a compound heterozygote for two seemingly severe mutations: a mutation of the intron 1 splice-donor site (GT→TT, the same mutation as was seen in PBD006) and a 2-bp deletion, in exon 1, that would be expected to encode a truncated protein containing only the first eight amino acids of PEX12, followed by six additional amino acids (fig. 3 and table 1).

Characterization of PEX12 *mRNA in PBD099*

Because the mutations in PBD099 were inconsistent with the prevailing assumptions about phenotype-genotype relationships within the PBDs, we examined further the consequences of the *PEX12* mutations identified in PBD099. Of the two *PEX12* mutations in PBD099, the intron 1 splice donor–site mutation (GT→TT) is also present in PBD006, a severely affected ZS patient with no peroxisomal matrix protein import and very low levels of *PEX12* mRNA. This result alone indicated that the mild phenotypes of PBD099 arose from the second *PEX12* allele of PBD099 (c.26,27Δ). RT-PCR analysis supported the hypothesis that the c.26,27Δ allele expressed the predominant form of *PEX12* in PBD099 cells: *PEX12* cDNA was amplified from the RNA of PBD099, and direct sequence analysis revealed that it all had the c.26,27Δ mutation (fig. 4*A*). Furthermore, all of the *PEX12* cDNA amplified from the RNA of PBD099 appeared to be processed correctly (within the sensitivity limits of RT-PCR, direct sequence analysis, and agarose-gel electrophoresis), which indicates that the c.26,27Δ mutation did not induce aberrant processing of the *PEX12* transcript. Northern blot analysis also suggested normal *PEX12* mRNA size and abundance in PBD099 cells (fig. 2).

These data indicated that the c.26,27Δ mutation was incorporated into a significant majority, if not all, of the *PEX12* mRNA present in the PBD099 cells. However, it was also possible that the *PEX12* cDNA that we generated by RT-PCR did not reflect all of the *PEX12* mRNA in PBD099 cells. Our previous study of *PEX12*-gene structure had indicated that *PEX12* consists of just three exons, but we had not identified the 5′ end of the *PEX12* mRNA, which leaves open the possibility that additional exons exist in the 5′ region of the cDNA. Given that exon skipping can be induced by mutations such as those present on either of the *PEX12* alleles from PBD099 (Dietz et al. 1993), the presence of additional exons in the 5′ region would make it possible to bypass the c.26,27Δ mutation, by skipping the affected exon. Such *PEX12* mRNAs might also lack the 5′ oligonucleotide used for generating the *PEX12* cDNA by RT-PCR and would not be represented in *PEX12* cDNA from PBD099. Therefore, it was necessary to determine the 5′ end of the *PEX12* mRNA and to complete the analysis of *PEX12*-gene structure.

Using 5′ RACE, we obtained cDNA clones that extended the 5′ end of the *PEX12* cDNA an additional 519 bp upstream of the *PEX12* ORF, yielding a 5′ UTR of 537 bp (fig. 4*B*). Multiple 5′-RACE clones were identified, and all were approximately the same length. To determine whether any introns might spilt the 5′ UTR of *PEX12* into separate exons, we amplified the 5′ UTR of *PEX12* from control human cDNA and genomic DNA samples (fig. 4C). The presence of similarly sized products in both reactions demonstrated that the 5′ UTR of *PEX12* cDNA is colinear with the *PEX12* gene. The absence of any upstream introns allowed us to conclude that the 5′ oligonucleotide used for RT-PCR amplification of *PEX12* cDNA lies within exon 1 of the gene, as shown in figure 4*D*. Nevertheless, we again performed RT-PCR analysis of *PEX12* mRNA from PBD099 cells and from a control cell line from an unaffected individual, this time using a 5′ primer located near the 5′ end of the *PEX12* mRNA. Identically sized products were obtained from both reactions. Once again, all of the longer *PEX12* cDNA from PBD099 cells has the c.26,27Δ mutation but otherwise normal *PEX12* structure (data not shown).

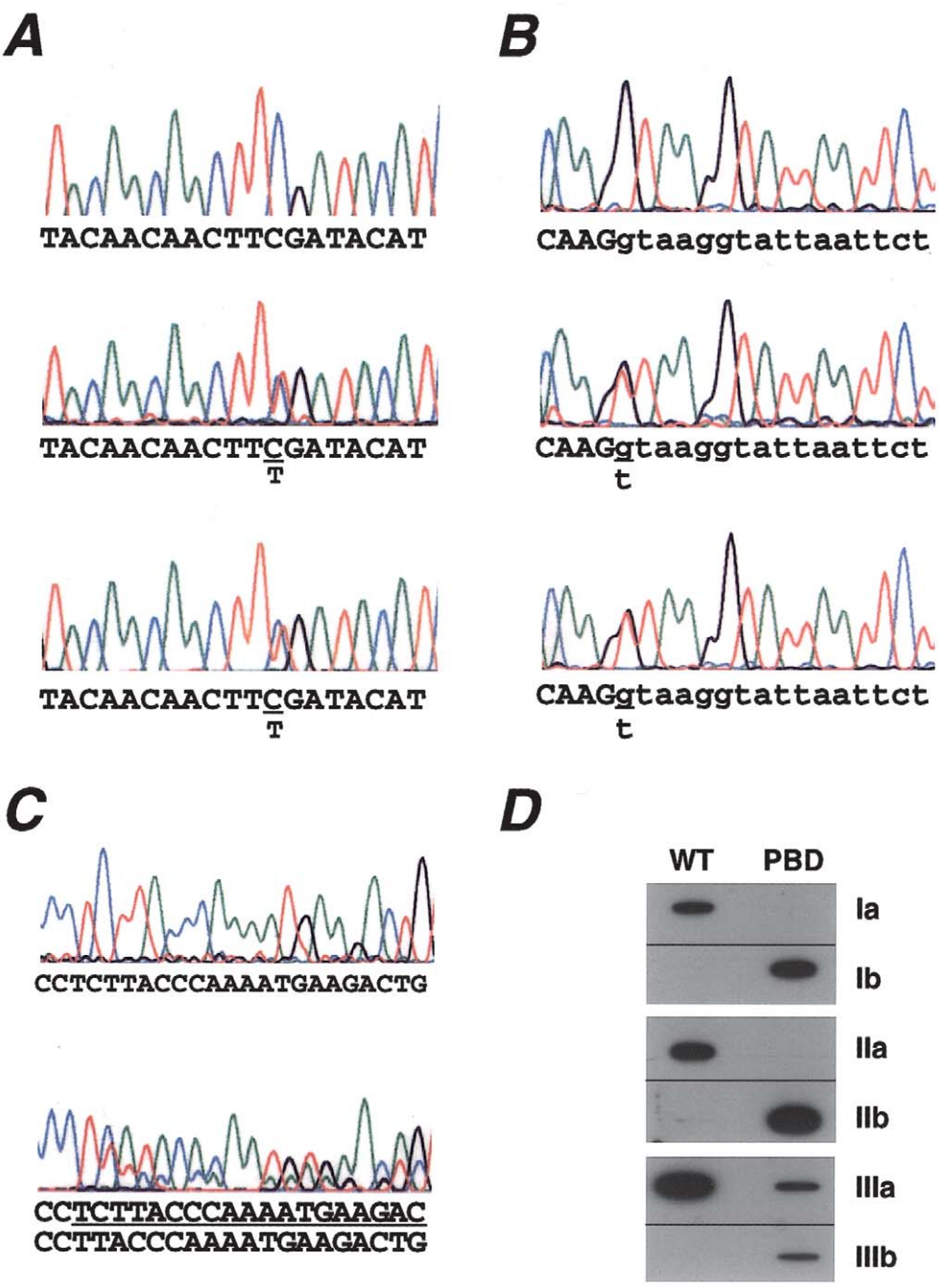

Figure 3 *PEX12* mutations in CG3 PBD patients. A 2.3-kb genomic DNA fragment spanning the *PEX12* gene was amplified from each of five CG3 patients and a control and either was sequenced directly or was subjected to ASO analysis. All PBD mutations are shown here, some by direct sequencing and others by ASO. *A,* Comparison of *PEX12* sequence over nucleotides 527–545 of the ORF from a control individual (*top*), PBD006 (*middle*), and PBD098 (*bottom*). Note that PBD006 and PBD098 are heterozygous for the CGA→TGA, R180ter mutation. *B, PEX12* sequence at the splice-donor site of intron 1 from a control individual (*top*), PBD006 (*middle*), and PBD099 (*bottom*). Intronic sequences are shown as lowercase letters. *C, PEX12* sequence over nucleotides 885–907 of the *PEX12* ORF from a control individual (*top*) and PBD098 (*bottom*), who is heterozygous for a 2-bp deletion (TC). The resulting differences are underlined. *D,* ASO-hybridization analysis of *PEX12* mutations. Each panel shows autoradiograms of slot blots in which the *PEX12* gene from control and PBD CG3 patients was hybridized with radiolabeled oligonucleotides. Each panel represents two filters, with the control DNA on the left and with the patient DNA on the right (filters Ia and Ib, PBD095 genomic DNA; filters IIa and IIb, PBD096 genomic DNA; filters IIIa and IIIb, PBD099 genomic DNA). In each panel, the upper filter (*a*) was hybridized with the control oligonucleotide, and the lower filter (*b*) was hybridized with the mutant oligonucleotide. Note that PBD006, PBD098, and PBD099 are compound heterozygotes, whereas PBD095 and PBD096 are homozygous for their mutations.

Table 1

Summary of Clinical Phenotypes, Peroxisome Protein Import Properties, and *PEX12* Gene Structures of PBD CG3 Patients

Cell Line	Clinical Phenotype	Life Span	PTS1-Protein Import	PTS2-Protein Import	*PEX12* mRNA Level (%)	Mutation(s)	Predicted Consequence of Mutation
PBD006	ZS	3 mo	−	−	14	GT→TT at splice donor site of intron 1	Aberrant splicing
						538C→T	R180ter
PBD040	ZS	3 mo	−	−	92	684–687delTAGT	Frameshift
PBD095	NALD	>4 years	+	+	48	202–204delCTT	L68Δ
PBD096	ZS	Unknown	−	−	34	268–271delAAGA	Frameshift
PBD097	ZS	1 mo	−	−	60	733–734insGCCT	Frameshift
						744–745insT	
PBD098	ZS	1 mo	−	−	29	538C→T	R180ter
						887–888delTC	Frameshift
PBD099	IRD	>23 years	+++	+++	70	26–27delCA	Frameshift
						GT→TT at splice-donor site of intron 1	Aberrant splicing
GM5756	Unaffected		+++++	+++++	100		

Activity of the PEX12*/c.26,27Δ cDNA*

The fact that the c.26,27Δ mRNA was the predominant *PEX12* mRNA present in PBD099 cells indicated that it was responsible for the mild phenotypes of this patient. This hypothesis was tested directly by means of the *PEX12* functional complementation assay (Chang et al. 1997). A *PEX12*-deficient cell line, PBD097 (table 1), was transfected with vectors designed to express C-terminally myc-tagged derivatives of the wild-type and c.26,27Δ *PEX12* cDNAs (we have demonstrated previously that addition of the myc tag to the C-terminus of PEX12 does not affect its activity; Chang et al. 1997). After 2 d of incubation, the transfected cell populations were processed for indirect immunofluorescence and were examined to determine the percentage of cells importing peroxisomal matrix proteins and expressing PEX12myc. These data revealed that the *PEX12myc*/c.26,27Δ cDNA displayed significant *PEX12* activity that was $\sim \frac{1}{7}$ that of the wild-type expression vector (table 2). This level of activity is similar to that reported for a mild allele of *PEX1* that also results in the IRD phenotype (Reuber et al. 1997). Thus, the sole *PEX12* mRNA detected in PBD099 cells displays a level of *PEX12* activity that is consistent with the phenotypes of PBD099.

Products of the PBD099 c.26,27Δ Allele

The deduced product of the *PEX12*/c.26,27Δ mRNA consists of the first eight amino acids of the protein, a short peptide that is extremely unlikely to mediate *PEX12* function. Therefore, we used an in vitro translation system to test the hypothesis that alternative PEX12 proteins might be produced from the *PEX12*/c.26,27Δ mRNA. Rabbit reticulocyte lysates containing [^{35}S]-methionine were charged with transcripts from the wild-type and c.26,27Δ *PEX12* cDNAs as well as with those from a truncated *PEX12* cDNA in which the first in-frame AUG corresponds to the codon for M94 (*PEX12*/1-93Δ). The *PEX12* ORF has several internal AUG codons (at nucleotides 30, 94, 118, 168, 220, 221, and 300), but the M94 AUG codon has the correct sequence context (i.e., gua.AUG.g) for high-efficiency translation initiation (Kozak 1992). The products of these in vitro translation reactions were then analyzed after separation by SDS-PAGE. The deduced molecular mass of PEX12 is 39 kD, and the wild-type *PEX12* cDNA directed the synthesis of an ~40-kD protein (fig. 5*A*). However, the product of the *PEX12*/c.26,27Δ cDNA was ~29 kD, the size expected for a protein initiating at the M94 codon. The product of the *PEX12*/1-93Δ cDNA was also 29 kD (fig. 5*A*, lane 3).

The 29-kD product of the *PEX12*/c.26,27Δ mRNA could be generated only by translation initiation at an internal AUG codon. To test whether similarly sized proteins were generated from the c.26,27Δ allele, we utilized a gene-transfection assay (we have demonstrated elsewhere that the *PEX12* gene, complete with all intronic sequences, rescues the defects of *PEX12*-deficient cells as efficiently as does the *PEX12* cDNA; Chang et al. 1997). Human fibroblasts were transfected with plasmids designed to express C-terminally myc-tagged versions of the wild-type and c.26,27Δ *PEX12* genes. Two days after transfection, the products of each gene were detected by western blot analysis using anti-myc antibodies. Cells transfected with the *PEX12myc* gene contained full-length PEX12myc of the predicted size, ~40 kD (fig. 5*B;* the myc tag adds ~1 kD to the size of

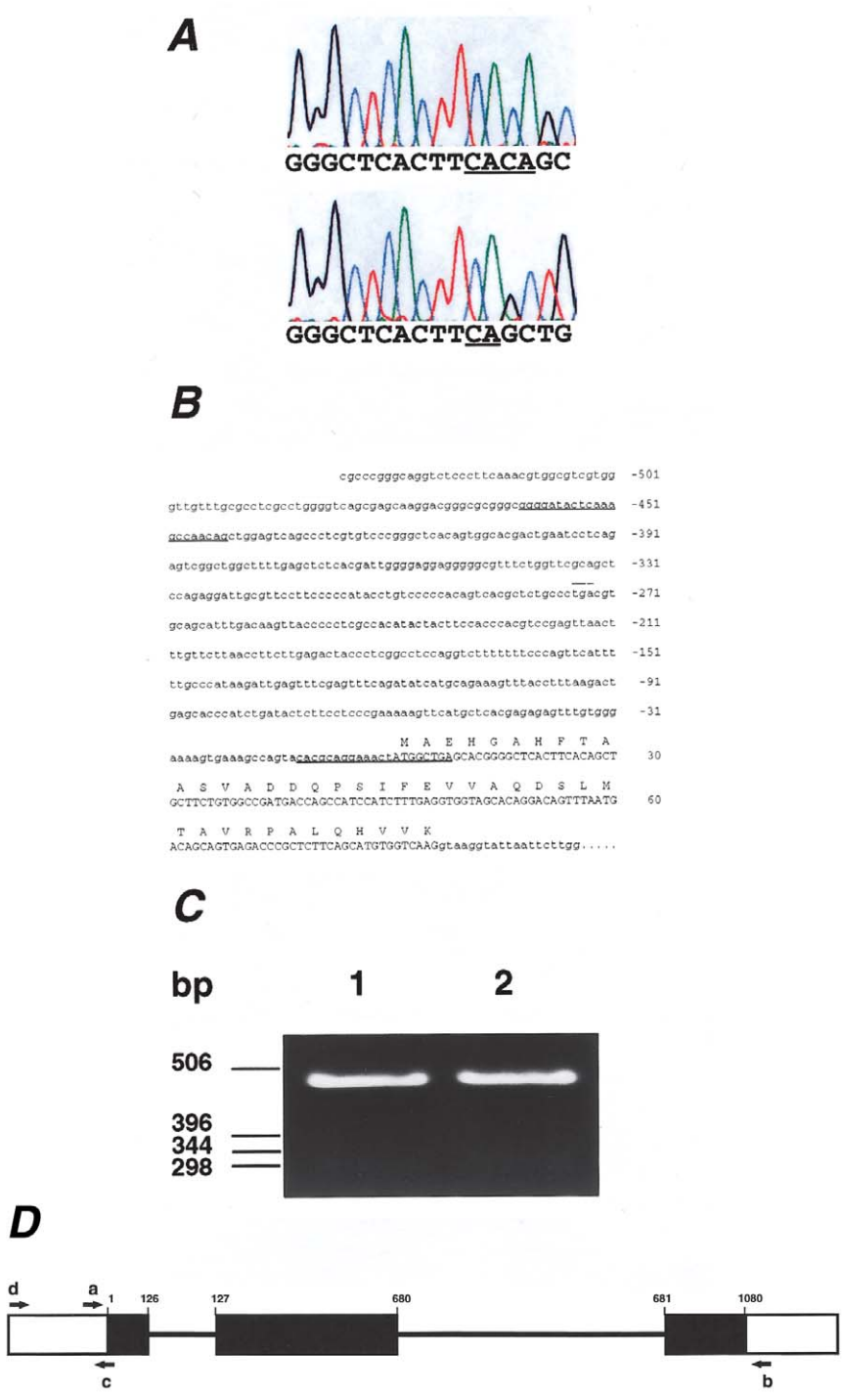

Figure 4 *PEX12* structure in normal and PBD099 cells. *A*, Direct sequence analysis of PBD099 cDNA. *PEX12* RNA from control cells and from PBD099 cells was converted to cDNA by RT-PCR using oligonucleotides flanking the *PEX12* ORF. Direct sequence analysis of the control *PEX12* cDNA (*top*) and PBD099 *PEX12* cDNA (*bottom*) revealed that all cDNA from PBD099 cells had the 2-bp deletion from the c.26,27Δ allele (conversion of CACA to CA). *B*, Sequence of *PEX12* exon 1, as deduced from 5′-RACE and genomic DNA analysis. The in-frame stop codon upstream of the *PEX12* ORF is overlined, and the underlined sequences correspond to the oligonucleotides used in panel *C*. *C*, Agarose-gel electrophoresis analysis of 5′-UTR amplification products. The products were generated with either cDNA (lane 1) or genomic DNA (lane 2) used as the template and with the oligonucleotides underlined in panel *B* used as primers. *D*, Diagram of transcribed segment of the *PEX12* gene. Blocks represent exonic sequences, and intervening lines represent the two *PEX12* introns. Blackened segments represent coding regions of the exons, whereas unblackened segments represent the 5′ UTR and 3′ UTR. Oligonucleotides used for amplification of the *PEX12* gene and cDNA fragments are represented as lines shown above and below the gene diagram. Oligonucleotides a and b (Chang-21 and Chang-20, respectively) were used for RT-PCR amplification of *PEX12* cDNA, as described in panel *A;* oligonucleotides d and c (Chang-120 and *PEX12* RACE-3′, respectively) were used for amplification of the *PEX12* 5′ UTR from both genomic DNA and cDNA, as described in panel *C;* oligonucleotides d and b were used for RT-PCR amplification of the 5′-UTR and ORF, as described in the text.

Table 2

In Vivo PEX12 Activities Expressed by Wild-Type and c.26,27Δ *PEX12myc*

PEX12myc Type	Expression[a] (%)	Activity[b] (%)	Normalized Activity[c]	Relative Rescue Activity[d] (%)
Wild type	9.79	49.45	5.05	100
26,27Δ	3.12	2.62	.84	16.63

[a] Proportion of myc-positive cells, among 1,500.
[b] Proportion of cells exhibiting catalase import, among 1,500.
[c] Calculated by dividing "Activity" by "Expression."
[d] Normalized activity as percentage of wild-type activity.

PEX12). In contrast, cells transfected with the *PEX12myc*/c.26,27Δ gene contained two shorter PEX12 proteins, ~30 and ~27 kD in size, the smaller of which was also synthesized from the wild-type gene; these proteins have the intact PEX12 C-terminus (the myc tag is located at this position) and have the size expected for proteins that initiate at the M94 and M118 AUG codons, respectively.

Discussion

The pioneering cell-fusion complementation studies of Brul et al. (1988) and Roscher et al. (1989) established that ZS, NALD, and IRD are genetically heterogeneous and that all three classes of patients could be found within a single CG. The simplest interpretation of these data is that the differences between ZS, NALD, and IRD patients are caused by differences in allele severity. Although the limited mutation studies reported in the initial characterizations of the *PEX2* (Shimozawa et al. 1992), *PEX6*(Fukuda et al. 1996; Yahraus et al. 1996), *PEX12*(Chang et al. 1997; Okumoto and Fujiki 1997), *PEX7*(Braverman et al. 1997; Motley et al. 1997; Purdue et al. 1997), *PEX1*(Portsteffen et al. 1997; Reuber et al. 1997), and *PEX10* (Warren et al. 1998) genes have provided anecdotal support to this hypothesis, there has yet to be a systematic analysis of phenotype-genotype correlations within any group of PBD patients.

In the present report, we have shown that both alleles of *PEX12* are mutated in all seven representatives of CG3 in our patient population, which confirms the earlier observation that mutations in *PEX12* are responsible for disease in CG3 of the PBD (Chang et al. 1997; Okumoto and Fujiki 1997). In CG3, the five ZS patients have the most pronounced clinical deficits, lack detectable matrix protein import, and have nonsense, frameshift, or splice-site mutations on both alleles of *PEX12*. The hypothesis that milder mutations in *PEX12* would result in less pronounced cellular and clinical phenotypes was supported by our analysis of PBD095. This NALD patient has relatively mild clinical phenotypes, including an extended life span (currently 4 years), and imports detectable amounts of PTS1 and PTS2 proteins. This individual is homozygous for an in-frame deletion of one codon, L68, which reduced but did not eliminate *PEX12* activity. However, PBD099 presented a paradox. PBD099 displayed the mildest clinical and cellular phenotypes of all CG3 patients but was a compound heterozygote for the following mutations, which would truncate the protein shortly after initiation: (1) a splice donor–site mutation in intron 1 and (2) a 2-bp frameshifting mutation in codon 9 of the *PEX12* ORF. The first of these mutations is also present in a ZS patient (PBD006) who contains little *PEX12* mRNA and displays a severe defect in peroxisomal matrix protein import. This result alone implicated the second PBD099 *PEX12* allele in the expression of detectable *PEX12* activity. This hypothesis was supported by two other observations. First, the only *PEX12* mRNA detected in PBD099 cells carried the c.26,27Δ mutation, and, second, the *PEX12*/c.26,27Δ cDNA had significant *PEX12* activity, ~ $\frac{1}{7}$ that of the wild-type cDNA. A similar decrease in *PEX*-gene activity is associated with the *PEX1*/G843D allele, a mutation that also results in IRD phenotypes (Reuber et al. 1997).

These data clearly implicate the *PEX12*/c.26,27Δ allele as the source of *PEX12* activity in PBD099. However, they do not explain how significant *PEX12* activity was generated from an mRNA that is predicted to encode just the first eight amino acids of PEX12, particularly in light of mutation data from other *PEX12*-deficient patients demonstrating that other regions of *PEX12* are critical for function. Therefore, we characterized further the protein products of the c.26,27Δ mRNA. In vitro translation studies demonstrated that the *PEX12*/c.26,27Δ mRNA directed the synthesis of a 29-kD protein, a product that could only be synthesized by translation initiation at an internal AUG codon. A protein of identical size was synthesized from a truncated *PEX12* mRNA in which M94 was the first in-frame start codon. Furthermore, the M94 codon is in the correct context (i.e., gua.AUG.g) for high-efficiency translation initiation. Gene-transfection studies also indicated that the c.26,27Δ allele could direct the synthesis of N-terminally truncated PEX12 proteins, adding further support to the hypothesis that *PEX12* activity may be generated by translation initiation at internal AUG codons along the *PEX12*/c.26,27Δ mRNA. However, it should be noted that we did not sequence the PEX12 protein(s) present in PBD099 cells. Therefore, it is formally possible that the truncated PEX12 proteins observed in the in vitro translation and in gene-transfection studies may have been generated by some unknown mechanism.

If it can be assumed that translation at one or more internal AUG codons is responsible for the synthesis of truncated PEX12 proteins from the c.26,27Δ allele, how

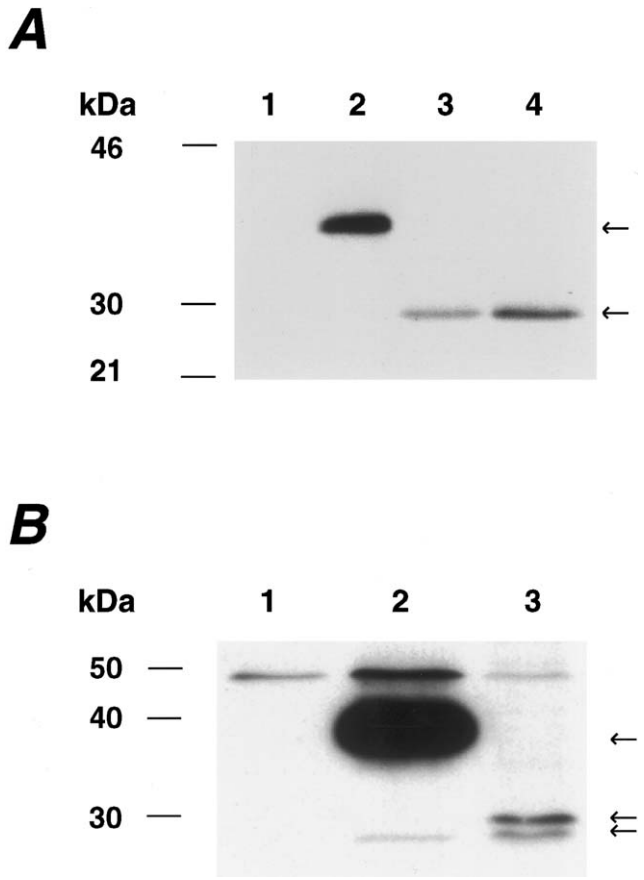

Figure 5 PEX12 products of the c.26,27Δ allele. The positions of molecular-weight markers are shown to the left of both panels. *A*, SDS-PAGE mobilities of in vitro–synthesized PEX12 proteins. Rabbit reticulocyte lysates were used to synthesize [^{35}S]-labeled products of *PEX12* cDNA (lane 2), *PEX12*/c.26,27Δ cDNA (lane 3), and *PEX12*/1-93Δ cDNA (lane 4). Equivalent portions of each sample were then separated by SDS-PAGE, and radiolabeled proteins were detected by fluorography. Lane 1 contained an equivalent amount of rabbit reticulocyte lysate. Arrows indicate the mobilities of the full-length PEX12 protein (*upper arrow*) and the product of the c.26,27Δ and 1-93Δ cDNAs (*lower arrow*). *B*, Proteins produced from the *PEX12myc* and *PEX12myc*/c.26,27Δ genes. Normal human skin fibroblasts were transfected with vector alone (lane 1) and with plasmids designed to express either the *PEX12myc* gene (lane 2) or the *PEX12myc*/c.26,27Δ gene (lane 3). Two days after transfection, cell lysates were prepared, separated by SDS-PAGE, and subjected to immunoblot analysis using polyclonal anti-myc antibodies. The two lowermost arrows to the right of the blot show the mobilities of myc-tagged proteins expressed from the *PEX12myc*/c.26,27Δ gene. The topmost arrow indicates the observed mobility of full-length PEX12myc. Note that the lower band produced from the *PEX12myc*/c.26,27Δ gene was also produced from the wild-type *PEX12myc* gene. All samples also had a reactive band of ~47 kD, which may be derived from the endogenous c-myc protein.

might this occur? Internal ribosome-entry sites have been identified in certain mammalian mRNAs, allowing translation at downstream AUGs. Such an element may precede M94 in the *PEX12* mRNA. However, it is also possible that truncated PEX12 proteins may be expressed through a termination/reinitiation mechanism such as that which occurs in certain viral and artificial polycistronic mRNAs of mammalian cells (Peabody and Berg 1986). In mammalian cells, expression by termination/reinitiation on polycistronic mRNAs is inefficient and can be greatly influenced by the relative position of the upstream and downstream ORFs of the mRNA (Peabody et al. 1986). It is interesting to note that a ZS patient (PBD096) who is homozygous for a frameshift mutation following codon 89 also has M94 as the first AUG in the ORF. However, the mRNA produced from the PBD096 alleles has a 4-bp deletion 8 bp upstream of M94 and fails to express detectable *PEX12* activity in vivo. If internal ribosome entry is responsible for expression of truncated PEX12 proteins in PBD099 cells, then the 4-bp deletion in PBD096 may disrupt the sequence required for internal translation initiation. Alternatively, if truncated PEX12 is synthesized by termination and subsequent reinitiation, the increased size and relative proximity of the upstream ORF in PBD096 may affect the reinitiation efficiency at either M94 or M118 and thus affect the ability to express *PEX12* function in PBD096 cells.

Translation initiation at internal AUG codons is rare but has been demonstrated for many genes. In addition to instances in which upstream AUG codons are normally skipped in favor of downstream start sites (Kozak 1989), termination and reinitiation on viral and artificial polycistronic mRNAs has been observed in mammalian cells (Peabody and Berg 1986), as has internal ribosome entry (McBratney et al. 1993; Belsham and Sonenberg 1996). Although we are unaware of any other instances in which this mechanism is thought to modulate human disease phenotypes, translation initiation at internal AUG codons along the murine androgen-receptor mRNA has been invoked to explain the relatively mild phenotypes of the *Tfm* mouse, a mutant caused by a nonsense mutation farther 5′ in the androgen-receptor gene (Gaspar et al. 1991). In view of our results with *PEX12* in PBD099, it may be that internal translation initiation should be considered when one is faced with the paradox of mild phenotypes and apparently severe mutations, particularly when the mutations lie early in the coding region of the disease gene.

In summary, we find that the relationship between genotype and phenotype in *PEX12*-deficient patients is relatively straightforward. Loss-of-function alleles appear to cause both severe defects in peroxisomal matrix protein import and severe clinical phenotypes, whereas alleles with partial *PEX12* activity lead to partial defects in protein import and relatively mild clinical phenotypes. The human *PEX12* gene has been cloned independently, and mutations for three PBD patients have been reported by Fujiki and colleagues (Okumoto and Fujiki 1997;

Okumoto et al. 1998). These include a K231ter mutation in PBD3-02 (Okumoto and Fujiki 1997), an S292ter mutation in PBD3-01, and an R180ter mutation in PBD3-03 (Okumoto et al. 1998), all of whom are thought, on the basis of analysis of RT-PCR-generated cDNAs from these patients, to be homozygotes. Interestingly, PBD3-03 is the same as patient PBD006 of this report, a compound heterozygote for the R180ter mutation and the intron 1 splice donor–site mutation that is also found in PBD099 cells. The inability of Okumoto et al. (1998) to detect cDNAs emanating from the allele with the intron 1 splice donor–site mutation lends independent support to the hypothesis that this allele cannot be expressed and thus that the c.26,27Δ allele is indeed the predominant form of *PEX12* expressed in PBD099 cells. Although we used different techniques for genotype and phenotype analysis than were used by Fujiki and colleagues, the fact that the latter group identified nonsense mutations (K231ter and S292ter) in ZS patients lends support to the hypothesis that severe mutations in *PEX12* lead to severe clinical phenotypes.

Acknowledgments

We thank Ann and Hugo Moser for the generous gift of skin fibroblasts from PBD patient, and we thank Cassandra Obie for aid in preparation of the northern blot analysis of the PBD patients. We extend our gratitude to other members of the Gould lab and to David Valle for helpful comments during the course of this work. This study was supported by National Institutes of Health grants DK45787 and HD10891 to S. J. G.

Electronic-Database Information

Accession numbers and URLs for data in this article are as follows:

GenBank, http://www.ncbi.nlm.nih.gov/Web/Genbank (for *PEX12* cDNA and genomic DNA sequences [accession numbers U91521 and U91522])

References

Belsham GJ, Sonenberg N (1996) RNA-protein interactions in regulation of picornavirus RNA translation. Microbiol Rev 60:499–511

Braverman N, Steel G, Obie C, Moser A, Moser H, Gould SJ, Valle D (1997) Human PEX7 encodes the peroxisomal PTS2 receptor and is responsible for rhizomelic chondrodysplasia punctata. Nat Genet 15:369–376

Brul S, Westerveld A, Strijland A, Wanders RJA, Schram AW, Heymans HSA, Schutgens RBH, et al (1988) Genetic heterogeneity in the cerebrohepatorenal (Zellweger) syndrome and other inherited disorders with a generalized impairment of peroxisomal functions—a study using complementation analysis. J Clin Invest 81:1710–1715

Chang C-C, Lee W-H, Moser HW, Valle D, Gould SJ (1997) Isolation of the human PEX12 gene, mutated in group 3 of the peroxisome biogenesis disorders. Nat Genet 15:385–388

de Vet ECJM, van den Broek BTE, van den Bosch H (1997) Nucleotide sequence of human alkyl-dihydroxyacetonephosphate synthase cDNA reveals the presence of a peroxisomal targeting signal 2. Biochim Biophys Acta 1346: 25–29

Dietz HC, Valle D, Francomano CA, Kendzior RJ, Pyeritz RE, Cutting GR (1993) The skipping of constitutive exons in vivo induced by nonsense mutations. Science 259:680–683

Dodt G, Braverman N, Wong C, Moser A, Moser HW, Watkins P, Valle D, et al (1995) Mutations in the PTS1 receptor gene, PXR1, define complementation group 2 of the peroxisome biogenesis disorders. Nat Genet 9:115–124

Dyer JM, McNew JA, Goodman JM (1996) The sorting sequence of the peroxisomal integral membrane protein PMP47 is contained within a short hydrophilic loop. J Cell Biol 133:269–280

Evan GE, Lewis GK, Ramsay G, Bishop JM (1985) Isolation of monoclonal antibodies specific for human c-myc proto-oncogene product. Mol Cell Biol 5:3610–3616

Fukuda S, Shimozawa N, Suzuki Y, Zhang Z, Tomatsu S, Tsukamoto T, Hashiguchi N, et al (1996) Human peroxisome assembly factor-2 (PAF-2): a gene responsible for group C peroxisome biogenesis disorder in humans. Am J Hum Genet 59:1210–1220

Gaspar ML, Meo T, Bourgarel P, Guenet JL, Tosi M (1991) A single base deletion in the Tfm androgen receptor gene creates a short-lived messenger mRNA that direct internal translation initiation. Proc Natl Acad Sci USA 88: 8606–8610

Gould SJ, Keller GA, Hosken N, Wilkinson J, Subramani S (1989) A conserved tripeptide sorts proteins to peroxisomes. J Cell Biol 108:1657–1664

Gould SJ, Krisans S, Keller GA, Subramani S (1990) Antibodies directed against the peroxisomal targeting signal of firefly luciferase recognize multiple mammalian peroxisomal proteins. J Cell Biol 110:27–34

Grant SG, Jessee J, Bloom FR, Hanahan D (1990) Differential plasmid rescue from transgenic mouse DNAs into *Escherichia coli* methylation-restriction mutants. Proc Natl Acad Sci USA 87:4645–4649

Jansen GA, Ofman R, Ferdiandusse S, Ijlst L, Muijsers AO, Skjeldal OH, Stokke O, et al (1997) Refsum disease is caused by mutations in the phytanoyl-CoA hydroxylase gene. Nat Genet 17:190–193

Kozak M (1989) The scanning model for translation: an update. J Cell Biol 108:229–241

——— (1992) Regulation of translation in eukaryotic systems. Ann Rev Cell Biol 8:197–225

Lazarow PB, Moser HW (1995) Disorders of peroxisome biogenesis. In: Scriver C, Beaudet A, Sly W, Valle D (eds) The metabolic and molecular bases of inherited disease. McGraw-Hill, New York, pp 2287–2324

Maquat LE (1995) When cells stop making sense: effects of nonsense codons on RNA metabolism in vertebrate cells. RNA 1:453–465

McBratney S, Chen CY, Sarnow P (1993) Internal initiation of translation. Curr Opin Cell Biol 5:961–965

Michaud J, Brody L, Steel G, Fontaine G, Martin L, Valle D, Mitchell G (1992) Strand-separating conformational polymorphism (SSCP) analysis: efficacy of detection of point mutations in the human ornithine-d-aminotransferase gene. Genomics 13:389–394

Mihalik S, Morrell J, Kim D, Sacksteder K, Watkins P, Gould S (1997) Identification of PAHX as a Refsum disease gene. Nat Genet 17:185–189

Moser A, Rasmussen M, Naidu S, Watkins P, McGuinness M, Hajra A, Chen G, et al (1995) Phenotype of patients with peroxisomal disorders subdivided into sixteen complementation groups. J Pediatr 127:13–22

Motley AM, Hettema EH, Hogenhout EM, Brittes P, ten Asbroek ALMA, Wijburg FA, Baas F, et al (1997) Rhizomelic chondrodysplasia punctata is a peroxisomal protein targeting disease caused by a non-functional PTS2 receptor. Nat Genet 15:377–380

Okumoto K, Fujiki Y (1997) *PEX12* encodes an integral membrane protein of peroxisomes. Nat Genet 17:265–266

Okumoto K, Shimozawa N, Kawai A, Tamura S, Tsukamoto T, Osumi T, Moser H, et al (1998) *PEX12,* the pathogenic gene of group III Zellweger syndrome: cDNA cloning by functional complementation on a CHO cell mutant, patient analysis, and characterization of PEX12p. Mol Cell Biol 18: 4324–4336

Peabody DS, Berg P (1986) Termination-reinitiation occurs in the translation of mammalian cell mRNAs. Mol Cell Biol 6:2695–2703

Peabody DS, Subramani S, Berg P (1986) Effect of upstream reading frames on translation efficiency in simian virus 40 recombinants. Mol Cell Biol 6:2704–2711

Poll-The BT, Roels F, Ogier H, Scotto J, Vamecq J, Schutgens RBH, Wanders RJA, et al (1988) A new peroxisomal disorder with enlarged peroxisomes and a specific deficiency of acyl-CoA oxidase (pseudo–neonatal adrenoleukodystrophy). Am J Hum Genet 42:422–434

Portsteffen H, Beyer A, Becker E, Epplen C, Pawlak A, Kunau W-H, Dodt G (1997) Human PEX1 is mutated in complementation group 1 of the peroxisome biogenesis disorders. Nat Genet 17:449–452

Purdue PE, Zhang JW, Skoneczny M, Lazarow PB (1997) Rhizomelic chondrodysplasia punctata is caused by deficiency of human PEX7 a homologue of the yeast PTS2 receptor. Nat Genet 15:381–384

Reuber BE, Germain Lee E, Collins CS, Morrell JC, Ameritunga R, Moser HW, Valle D, et al (1997) Mutations in PEX1 are the most common cause of the peroxisome biogenesis disorders. Nat Genet 17:445–448

Roscher AA, Hoefler S, Hoefler G, Paschke E, Paltauf F, Moser A, Moser H (1989) Genetic and phenotypic heterogeneity in disorders of peroxisome biogenesis: a complementation study involving cell lines from 19 patients. Pediatr Res 26: 67–72

Shimozawa N, Suzuki Y, Orii T, Moser A, Moser HW, Wanders RJA (1993) Standardization of complementation grouping of peroxisome-deficient disorders and the second Zellweger patient with peroxisomal assembly factor-1 (PAF-1) defect. Am J Hum Genet 52:843–844

Shimozawa N, Tsukamoto T, Suzuki Y, Orii T, Shirayoshi Y, Mori T, Fujiki Y (1992) A human gene responsible for Zellweger syndrome that affects peroxisome assembly. Science 255:1132–1134

Slawecki M, Dodt G, Steinberg S, Moser AB, Moser HW, Gould SJ (1995) Identification of three distinct peroxisomal protein import defects in patients with peroxisomal biogenesis disorders. J Cell Sci 108:1817–1829

Subramani S (1993) Protein import into peroxisomes and biogenesis of the organelle. Annu Rev Cell Biol 9:445–478

Suzuki Y, Jiang LL, Souri M, Miyazawa S, Fukuda S, Zhang Z, Une M, et al (1997) D-3- hydroxyacyl-CoA dehydratase/ D-3-hydroxyacyl-CoA dehydrogenase bifunctional protein deficiency: a newly identified peroxisomal disorder. Am J Hum Genet 61:1153–1162

Swinkels BW, Gould SJ, Bodnar AG, Rachubinski RA, Subramani S (1991) A novel, cleavable peroxisomal targeting signal at the amino-terminus of the rat 3-ketoacyl-CoA thiolase. EMBO J 10:3255–3262

van der Klei IJ, Veenhuis M (1997) Yeast peroxisomes: function and biogenesis of a versatile cell organelle. Trends Microbiol 5:502–509

Warren DS, Morrell JC, Moser HW, Valle D, Gould SJ (1998) Identification of *PEX10,* the gene defective in complementation group 7 of the peroxisome-biogenesis disorders. Am J Hum Genet 63:347–359

Yahraus T, Braverman N, Dodt G, Kalish JE, Morrell JC, Moser HW, Valle D, et al (1996) The peroxisome biogenesis disorder group 4 gene, *PXAAA1,* encodes a cytoplasmic ATPase required for stability of the PTS1 receptor. EMBO J 15:2914–2923